

Self-Assembly of Functional Nanosurfaces and Complex Nanostructures with Genetically Modified Tobacco Mosaic Virus

Nicholas Horelik

Senior Honors Thesis, Tufts University, 04/20/2009

Abstract

In this project I explored two different methods for utilizing genetically modified tobacco mosaic viruses (TMVs) to robustly create tunable and functional nano-scale surfaces and structures. As highly stable nano-scale rods, TMVs provide for excellent nanotemplates that are programmable via nucleic acid hybridization and functionalizable with genetically inserted thiol groups in cysteine residues. Utilizing gold-thiol binding and functionalization with fluorescein, fluorescence and atomic force microscopy (AFM) results clearly demonstrate the capacity for TMVs to specifically and tunably self-assemble onto gold surfaces while retaining thiol functionality. Utilizing the hybridization-based assembly of TMVs to DNA miniarrays, AFM results should also clearly demonstrate the capacity for TMVs to be selectively linked to form TMV dimers, trimers, and other arbitrarily complex geometries, although no conclusive results were obtained prior to the submission of this document. Either of these two methods might find applications in producing better catalysts, providing more functionality to sensing surfaces, or lending strength or functionality to nano-scale devices.

Table of Contents

1. Introduction	1
1.1 Motivation and Goal	1
1.2 Background	1
2. Materials and Methods.....	3
2.1 Gold-Thiol Surface Assembly	3
2.1.1 Chip Preparation	3
2.2.2 Monolayer Assembly	4
2.2.3 Fluorescein Functionalization	4
2.2.4 Palladium Metallization	4
2.2.5 Fluorescence and Atomic Force Microscopy	5
2.3 DNA Hybridization.....	6
2.3.1 Monomer Creation and Assembly	7
2.3.2 Visualization	8
3. Results and Discussion	9
3.1 Gold-Thiol Surface Assembly	9
3.1.1 Fluorescence Microscopy Results	9
3.1.2 Atomic Force Microscopy Results.....	10
3.1.3 Palladium Metallization Results.....	12
3.2 DNA Hybridization.....	13
3.2.1 Difficulties	13
3.2.3 Suggestions	14
5. Conclusions	15
6. Appendix	16
7. Works Cited.....	17

1. Introduction

1.1 Motivation and Goal

In recent years research in nanotechnology has increased due to the many potential applications for nano-scale materials and structures. For example, nanostructures have a significantly larger surface area to volume ratio, thus suggesting a significant potential use as a support for catalysis by reducing the overall amount of precious metal required. Additionally, nanostructures hold the potential to introduce dramatic weight reductions and improved performance with applications in renewable energy, electronics, computing, diagnostics, medicine, and analytical chemistry⁽¹⁾⁽²⁾⁽³⁾⁽⁴⁾⁽⁵⁾⁽⁶⁾. However, difficulties arise when attempting to produce structures and surfaces on the nano-scale because nanoparticles tend to aggregate and can be very difficult to purify and use in a targeted fashion. In light of this, the goal of this project is to establish a targetable and robust building block for hierarchically assembling structures and surfaces across the nanometer and micrometer length scales, while demonstrating its potential application for use in catalysis. The chosen building block to explore is a genetically modified version of the Tobacco Mosaic Virus, as it has shown the potential to be used in this fashion in the past, for example in digital memory storage and battery electrodes⁽⁷⁾⁽⁸⁾⁽⁹⁾. Using nucleic acid hybridization as the targeting mechanism, complex structures made from this virus have many potential applications in hierarchical assembly in conjunction with DNA-based bottom-up fabrication techniques⁽¹⁰⁾, perhaps for example as a nanoswitch when metalized with a ferromagnetic metal⁽¹¹⁾.

1.2 Background

The Tobacco Mosaic Virus (TMV) is a 300nm long and 18nm in diameter nanorod consisting of approximately 2130 identical coat proteins helically positioned around a 6.4kb positive strand of genomic mRNA, giving it a 4nm in diameter inner channel (see Figure 1).

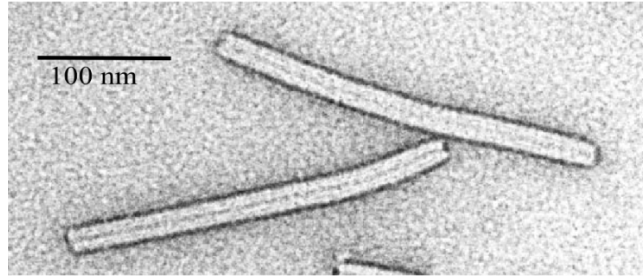


Figure 1 TEM image of WT TMV stained with uranyl ions, which appear black⁽¹²⁾.

The TMV virion is remarkably stable at temperatures of up to 90°C, in extreme pHs (2-10), and in a variety of organic solvents⁽¹²⁾⁽¹³⁾⁽¹⁴⁾. The virus also possesses a unique disassembly mechanism normally used for replication that entails the removal of coat proteins at the 5' end of the viral RNA⁽¹⁵⁾. By mimicking the conditions that normally occur when inside an infected plant cell we can induce this disassembly and then attach a complementary single stranded DNA for subsequent programmable targeting⁽¹⁶⁾. These properties combined with the ability to employ site directed mutagenesis to display specific amino acids on the surface of each coat protein⁽¹⁷⁾⁽¹⁸⁾⁽¹⁹⁾ make this virus an ideal candidate as a nano-scale building block. For this study, two such genetically modified TMV types were used, denoted TMV1cys and TMV98cys for the location on the polypeptide chain where a cysteine residue has been introduced (see Figure 2).

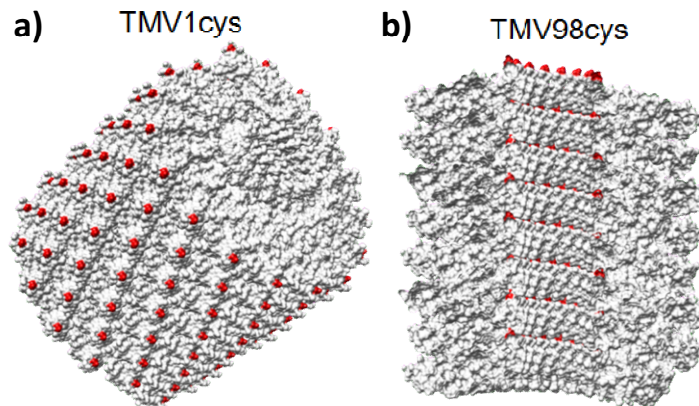


Figure 2 Models of TMV1cys and TMV98cys representing approximately 10% of the overall TMV length. Red dots indicate the location of genetically inserted cysteine residues. In a) TMV1cys, the residues are located at the 1st position on the outer portion of the TMV nanorod. In b) the cross section cut-away of TMV98cys, the residues are located along the 4nm diameter inner channel, and also extrude out at the 3' end of the virus.

2. Materials and Methods

2.1 Gold-Thiol Surface Assembly

Self-assembled monolayers were created on gold surfaces using TMV1cys and TMV98cys and then were subsequently functionalized with fluorescein or used for selective palladium metal deposition (see Figure 3). Samples were created from cut and cleaned gold wafers (either bare gold or gold-silicon patterned), and then analyzed via Atomic Force Microscopy (AFM) and/or fluorescence microscopy.

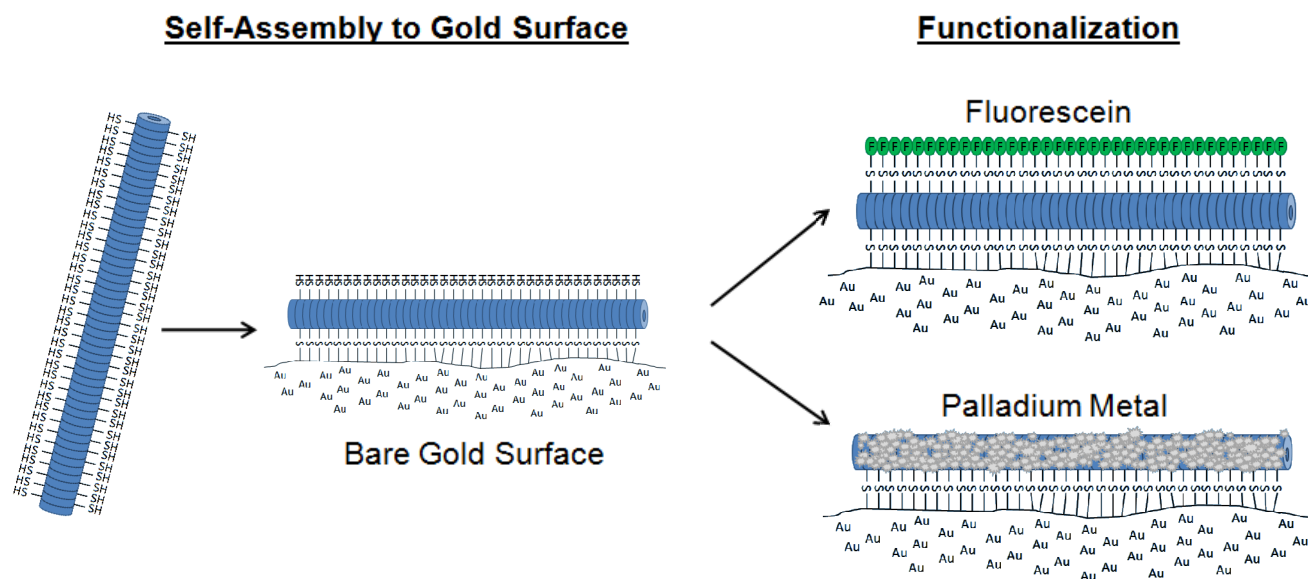


Figure 3 Schematic diagram of TMV self-assembly procedure. As shown here, sulfhydryl groups on the outer coat proteins of TMV1cys bind the virus to a gold surface and then are available for subsequent chemical modification or as reductive metallization nucleation sites.

2.1.1 Chip Preparation

Rectangular chips were cut from gold wafers so as to fit inside 2ml microcentrifuge tubes. To remove the photo-resist layer, the pieces were stirred for 20 minutes in each of acetone, isopropanol, and methanol. Subsequently, as the final step immediately before monolayer creation, all chips were etched in air plasma for 3 minutes at approximately 10mA. Chips that were previously subjected to TMV virions

were reused after incubation for 20 minutes each in concentrated sulfuric acid, bleach, and sodium hydroxide, followed again by plasma etching.

2.2.2 Monolayer Assembly

Immediately following plasma etching, gold chips were placed in 2ml microcentrifuge tubes filled with 1ml of TMV solution at variable concentrations in 2x SSC either with or without 0.01% Tween 20, and then incubated at room temperature overnight. Chips were then rinsed in 5ml Petri dishes for 20 minutes each of pH 7.0 PBS, Tris, and 2x SSC buffers, as well as de-ionized water, followed by drying under ultrapure N₂.

2.2.3 Fluorescein Functionalization

After rinsing but before drying, TMV-gold chips were placed in 2ml microcentrifuge tubes filled with 500µl pH 7.0 Tris buffer, and Fluorescein-5-Maleimide was added to a 10-fold molar excess. The tubes were covered with tinfoil to incubate in darkness for 30 minutes, and then were rinsed in de-ionized water for 10 minutes before drying under ultrapure N₂.

2.2.4 Palladium Metallization

After rinsing but before drying, TMV-gold chips prepared with 100ug/ml TMV1cys with 0.01% Tween 20 were placed in 2ml microcentrifuge tubes and filled with 1ml of freshly-made 2mM palladium tetrachlorate in a 30mM sodium hypophosphite solution. These chips were incubated in darkness for 20 minutes and briefly rinsed twice with 1ml de-ionized water in a separate microcentrifuge tube. For some chips, further reduction was achieved with the addition of dimethylaminoborane to 30mM, which was added directly to the palladium tetrachlorate incubation tubes for an additional incubation of 3 minutes.

2.2.5 Fluorescence and Atomic Force Microscopy

Fluorescein-modified TMV surfaces were visualized via excitation at 480nm in an Olympus BX51 microscope. AFM images were obtained using a Dimension 3100 atomic force microscope with a Nanoscope IV controller operated in dry tapping mode at approximately 300 Hz with Tap300 silicon probes.

2.3 DNA Hybridization

Controlled construction was attempted with TMV98cys by taking advantage of TMV's inner RNA and the sulfhydryl groups at the 98th position of each coat protein (see Figure 4). This project is still underway, having yet to produce reliable results.

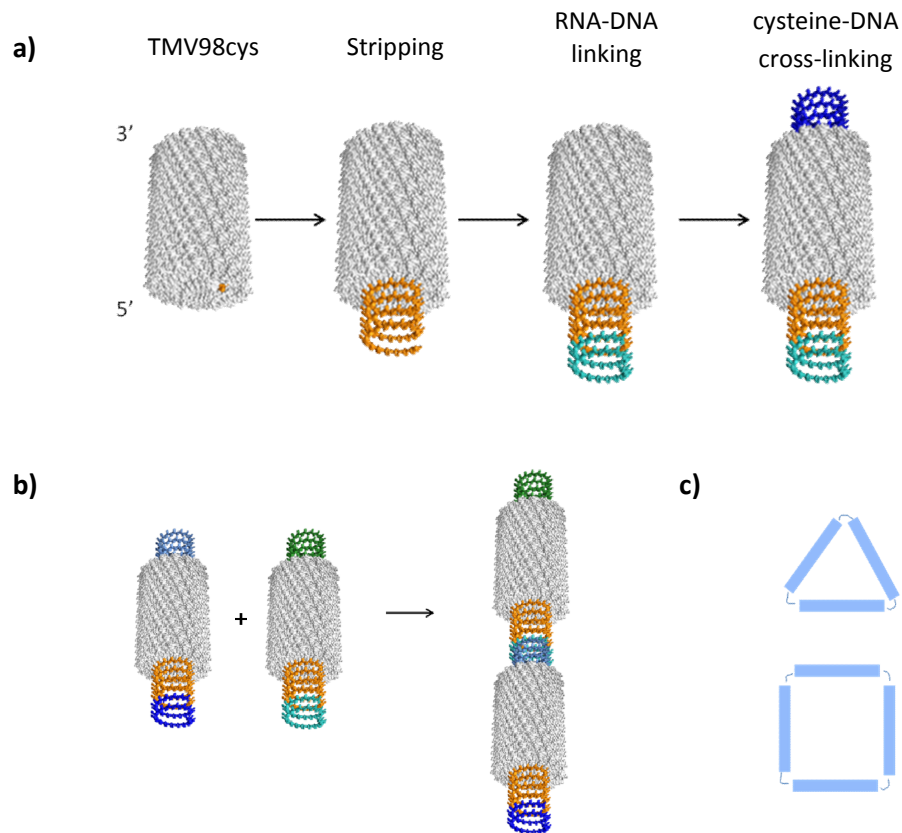


Figure 4 Schematic diagram of the proposed plan to use TMV98cys as a nano-scale building block which is targetable via nucleic acid hybridization. a) Coat proteins of TMV98cys are stripped away at the 5' end via gradient centrifugation, and then a custom single stranded DNA (light blue) is hybridized to the revealed viral RNA (orange). At the 3' end of the virus (the only location where the sulfhydryl groups at the 98th position are available for modification) an amine terminated single stranded DNA (dark blue) is attached with a heterobifunctional cross-linker. b) and c) Different custom monomers as produced in a) can be made into dimers, trimers, or other arbitrarily complex structures by matching complementary DNA strands.

2.3.1 Monomer Creation and Assembly

To create TMV monomers, TMV98cys in pH 8.0 Tris buffer was first separated by centrifugation in a 10-40% sucrose gradient at 48,000 g for 2 hours at 4°C to partially remove the coat proteins at the 5' end of the virus. These partially disassembled viruses were removed from the gradient, pelleted by centrifugation for 45 minutes at 106,000 g, and resuspended in 5xSSC. Next, single stranded (ss) “linker” DNA was hybridized with the exposed viral RNA for 2 hours at 30°C (see Table 1), and unbound ssDNA was removed by pelleting the mixture again by centrifugation for 45 minutes at 106,000 g in 5xSSC.

Table 1 Single stranded DNA sequences used for these experiments

Name	5' end	Sequence	3'end
Linker dnaK	-	<u>GTTTGTTGTTGTTGGTAATTGTTG</u> <i>TTTTTCTGGCAAACAACGCGAAAG</i> ¹	-
Probe dnaK	Amine	CTTTCGCGTTGTTGCAGAA	-
Linker 6xHis	-	<u>GTTTGTTGTTGTTGGTAATTGTTG</u> <i>TTTTTCATCATCATCATCAT</i> ¹	-
Probe 6xHis	Amine	ATGATGATGATGATGATG	-
Link 6xHis	Amine	CATCATCATCATCAT	-

¹ Constitutes the TMV 5' complementary sequence, a *spacer*, followed by the address specific sequence

For the final step in creating the monomer, 5' amine-terminated ssDNA (“probe”) was attached to the 3' end of the viruses by incubating the stripped and hybridized TMVs with 10-fold molar excess probe ssDNA and 1µl of 92mM sulfoSMPB (Sulfosuccinimidyl 4-[p-maleimidophenyl]butyrate) in 5xSSC buffer for 30 minutes. Unbound probe ssDNA was again removed by pelleting the mixture by centrifugation for 45 minutes at 106,000 g in 5xSSC, leaving a solution of TMV-DNA “monomers” as shown in Figure 4 a) after resuspension in 5xSSC. All subsequent hybridizations with these monomers to make more

complex structures were performed by combining each final monomer solution and then incubating for 2 hours at 30°C.

2.3.2 Visualization

It is intended to visualize dimers, trimers, and other structures made from TMV-DNA monomers by hybridizing such constructs to probe ssDNA chemically attached to an aldehyde functionalized glass slide in a DNA miniarray. Miniarrays were prepared as previously described⁽¹⁶⁾ with probe dnaK, probe 6xHis, link 6xHis, TMV5', and TMV3' as capture ssDNAs, and TMV constructs were hybridized overnight at 30°C in 5xSSC. Before drying with N₂ and visualization with AFM, slides were rinsed for 20 minutes at 30°C in each of 5xSSC with 0.01% Tween 20, 4xSSC, 3xSSC, and then at room temperature with 2xSSC and ultrapure water.

3. Results and Discussion

3.1 Gold-Thiol Surface Assembly

3.1.1 Fluorescence Microscopy Results

After binding TMV to patterned gold chips and functionalizing the free sulfhydryl groups with fluorescein-5-maleimide, samples were visualized under 480nm light to observe the location of TMV binding and confirm the accessibility of the free sulfhydryl groups for functionalization.

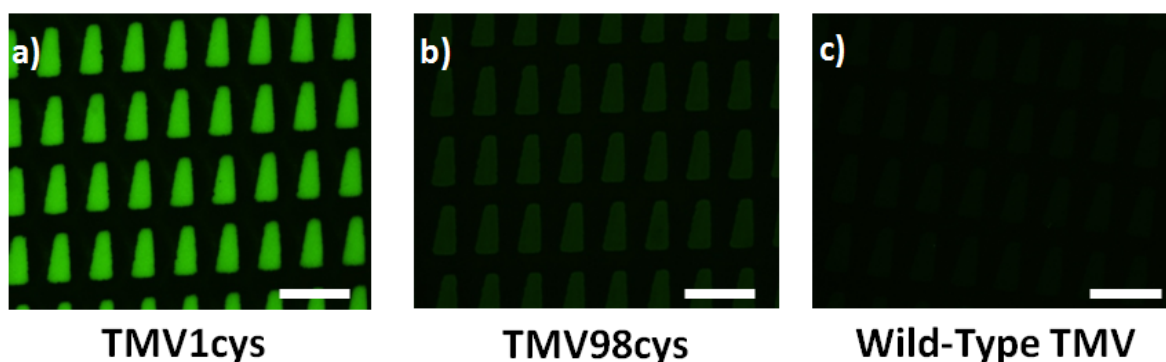


Figure 5 a) TMV1cys, b) TMV98cys, c) Wild-Type TMV all at 100μg/ml TMV in the binding solution on patterned gold (silicon oxide in between trapezoidal gold sections), functionalized with fluorescein. These chips were created with no Tween 20 present in the binding solution; when bound with Tween 20 fluorescence intensity for all chips is almost negligible. Scale bars represent 150 μm.

As seen in Figure 5, fluorescein was only found on the gold sections of the chips, and only in the presence of bound TMV1cys or TMV98cys. Also, in control experiments where TMVs were functionalized with fluorescein *before* attempted binding to gold, no significant fluorescence was observed, and few TMVs were seen with AFM (images not shown). These results demonstrate the precise preferential binding of these genetically modified TMVs to gold as well as show that this binding is the result of the added cysteine residues in the coat proteins of the TMV nanorods. Furthermore, it confirms the availability of sulfhydryl groups not involved in surface binding for functionalization after binding to gold. For TMV1cys these free sulfhydryl groups are on the outside of the nanorod, whereas

for TMV98cys they lie in the 4nm diameter inner channel. This difference in positioning is most likely what accounts for the difference in observed fluorescence intensity between Figure 5 a) and b). Also, given that the sulfhydryl groups of TMV98cys are only available for surface binding at the 3' end of the virus (compared to TMV1cys where they are along the entire length of the outside of the rod), there may also be less TMV98cys density on the surface (however, this is shown to be incorrect by the following AFM analysis). Regardless, overall this result confirms the efficacy of the gold-thiol binding method to accurately place these viruses on gold chips, with the availability of further functionalization.

3.1.2 Atomic Force Microscopy Results

The topological surface characteristics of the chips previously visualized with fluorescence microscopy were examined with AFM to confirm the previous results, check for uniformity of binding, and explore the extent to which the surface characteristics could be controlled. Immediately after checking for fluorescence, chips were visualized in dry tapping mode AFM.

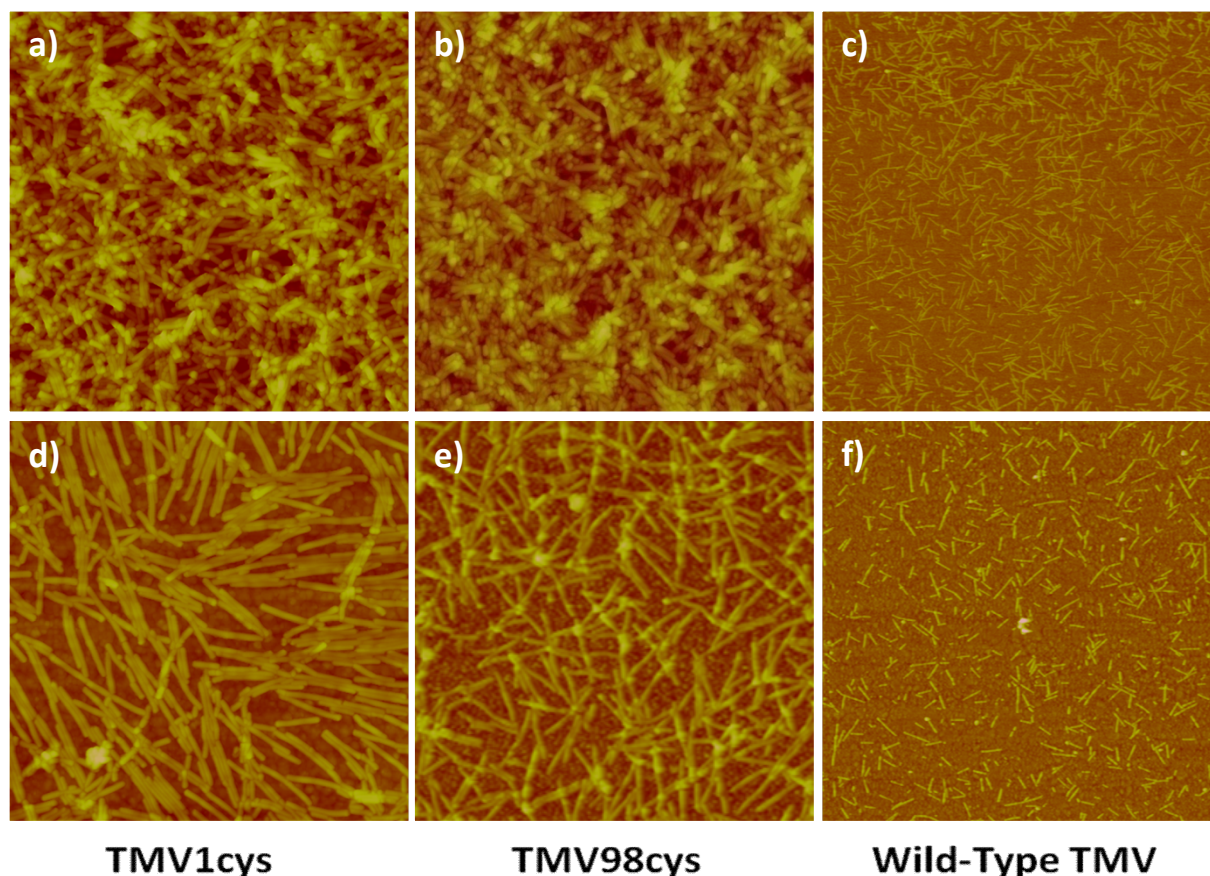


Figure 6 AFM images of TMV bound to the gold surfaces from Figure 5 (100μg/ml TMV binding solution). For the top row (a-c), TMV was bound to chips in the absence of Tween 20, and for the second row (d-f), TMV was bound in the present of 0.01% Tween 20, a simple surfactant. The first column (a,d) is TMV1cys, the second (b,e) TMV98cys, and the third (c,f) WT TMV. All images are 2μm×2μm except for c) and f), which are 10μm×10μm. See the appendix for expanded views of d) and e).

As seen in Figure 6, the density and orientation of viruses on the surface varies greatly with different binding conditions and virus type. For chips (d-f) bound in the presence of Tween 20, a simple surfactant, viral density is significantly less and a more ordered monolayer of viruses on the surface is created. For WT TMV, regardless of the presence on Tween 20, viral density is significantly low and comparable to viral density on the silicon oxide region of all chips (images not shown). These results confirm the conclusions drawn from the fluorescence microscopy as well as demonstrate the tunability of these surfaces. The genetically modified viruses do indeed show an increased binding capacity to gold over the WT, and the binding is indeed specific to gold over silicon oxide. As previously suggested, however, the density of TMV98cys bound without Tween 20 is not in fact less than that of TMV1cys.

Thus the decrease in fluorescence for these chips must be due to other reasons. For the case of the addition of Tween 20 to the binding solution, the viral density does in fact decrease, but the viruses assemble in a more ordered fashion. This probably happens because Tween 20 is able to separate viral aggregates known to occur in concentrated TMV solutions, allowing the viruses to bind one at a time as opposed to in large clumps. The end result is a more ordered self-assembled monolayer where viruses bind only to the surface via gold-thiol binding and not to each other via disulfide bonds. These surfaces can be further functionalized for novel applications, as explored in the next section.

3.1.3 Palladium Metallization Results

To demonstrate a potential application for these ordered self-assembled monolayers of viruses, palladium metal was deposited on the surfaces via reductive metallization, with the free sulfhydryl groups of TMV1cys acting as preferential nucleation sites for new metal clusters.

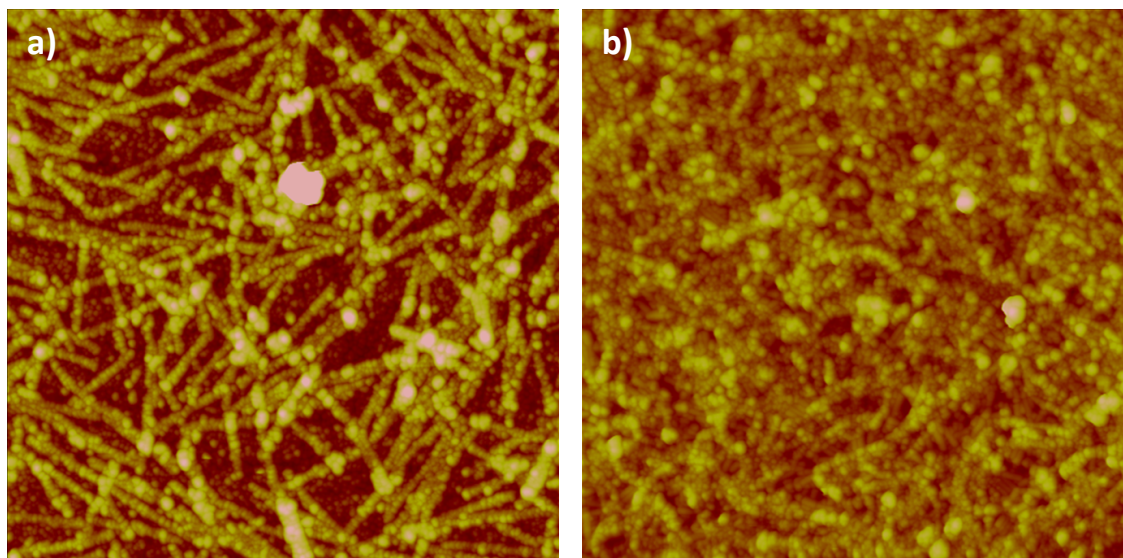


Figure 7 AFM images of TMV1cys bound to a gold chip a) in the presence of 0.01% Tween 20 and b) without Tween 20 after reductive palladium metallization. Images are 2 μ m \times 2 μ m. Compare to Figure 6 a) and d).

As seen in Figure 7, metal clusters can be clearly seen on the surfaces of the viruses. These palladium-coated virus surfaces can be used for catalysis, and indeed a study currently underway is yielding results using these chips for dichromate reduction. Given that the morphology and viral density of these TMV

surfaces can be controlled, and that the palladium reduction reaction can be tuned to yield bigger or smaller metal clusters, this result demonstrates the potential for these surfaces to provide a unique and powerful scaffold for a variety of applications, including catalysis.

3.2 DNA Hybridization

Unfortunately thus far the results for the DNA hybridization section of this project have been inconclusive, and efforts to improve the quality of the samples created have been unsuccessful. Several insights have indeed been garnered from the experiments carried out however, and it is expected that given more time and careful inspection that the fundamental concepts behind this project will indeed yield quality results.

3.2.1 Difficulties

Essentially thus far the difficulties encountered have been related to the DNA miniarray visualization method selected to view the results. Even after extensive rinsing as described in the methods section, nonspecific binding was observed everywhere on the DNA miniarray slides, even with WT viruses and unmodified viruses with no exposed RNA or DNA. However, this procedure has been previously shown to be successful⁽¹⁶⁾, so the issue may be something technical and small. As a results of these difficulties, even if the stripping, cross-linking, and hybridization is successfully creating viral dimers and trimers, they cannot be currently visualized in a way that conclusively demonstrates the intended construction. This is the case because of the natural end-to-end aggregation of these viruses in solution, and in particular with TMV98cys with sulfhydryl groups on the end to make disulfide bonds.

3.2.3 Suggestions

Several observations made in these initial attempts will help guide future efforts to modify the procedure to produce the desired results (see Table 2).

Table 2 Suggestions for improvement from observations of failed attempts.

No.	Variable to Modify <i>Suggestion</i>	Current Value of Variable	Notes
1	Amount of virus <i>Increase</i>	200ug TMV before stripping	- After the stripping centrifugation it is difficult to see the band of partially dissembled TMV - During each subsequent pelleting step TMV is lost (in some cases very little TMV was seen on the slide)
2	Centrifugation force <i>Decrease</i>	106,000g for unbound ssDNA removal	- Many times the pellet is too tightly attached to the wall of the centrifuge tube and does not completely resuspend. See procedure in (16)
3	Length of ssDNA <i>Increase</i>	18-20 bp	- May not provide flexible enough linkages for complex structures, increase to approximately 60 bp

It may also prove beneficial to switch to an entirely different method of visualization, such as binding to freshly-cleaved mica surfaces; however, in this case it may be difficult to differentiate natural TMV aggregation from hybridized linkages. In either case, length histograms should be used to compare samples and controls.

Once success is achieved in creating larger structures, further functionalization or metal deposition should also be demonstrated.

5. Conclusions

Despite the setbacks encountered in the second half of the project, the obtained results do indeed demonstrate the efficacy of using genetically modified tobacco mosaic viruses to create nano-scale functional surfaces. It is expected that further work on the DNA hybridization project will yield significant results, and further work is already being undertaken that builds off the surface binding results presented here. For example, others are working on platinum metallization, metal cluster size control with GISAXS and XPS analysis, as well as palladium-metalized TMV catalysis. Ultimately, this body of work lays the groundwork for a variety of other projects with a variety of potential applications.

6. Appendix

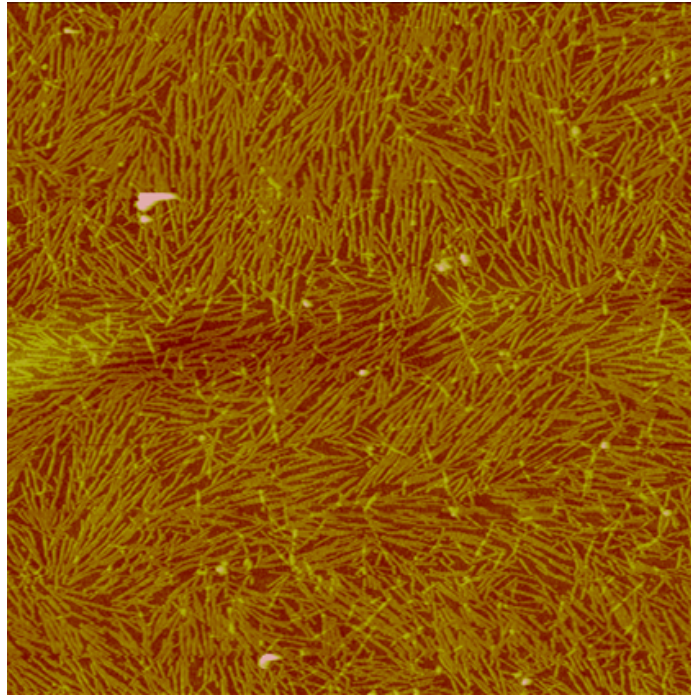


Figure 8 TMV1cys bound to gold surface in the presence of 0.01% Tween 20. Image is $10\mu\text{m} \times 10\mu\text{m}$

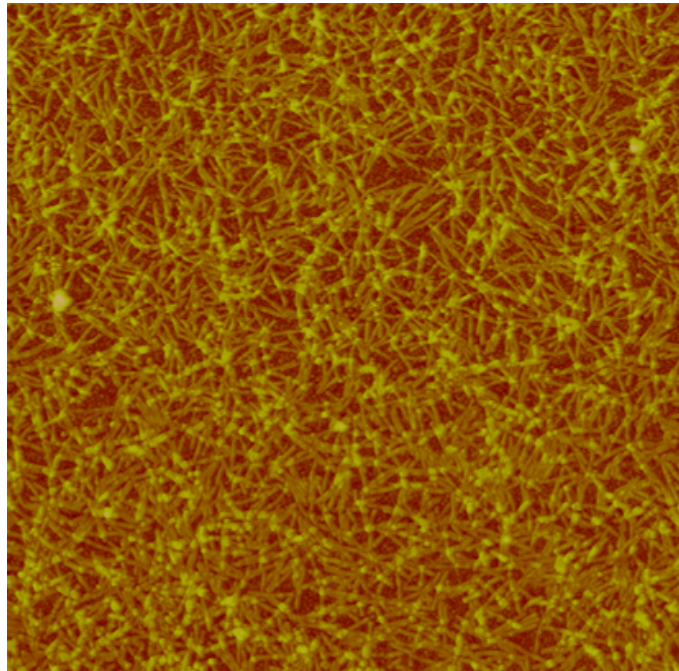


Figure 9 TMV98cys bound to gold surface in the presence of 0.01% Tween 20. Image is $5\mu\text{m} \times 5\mu\text{m}$

7. Works Cited

1. **Chomski, E. and Ozin, G.** 12, 2000, *Advanced Materials*, pp. 1071-1078.
2. **Correia, A., et al.** 204, 2007, *Phys. Status Solidi A*, pp. 1611-1622.
3. **Lehn, J.-M.** 295, 2002, *Science*, pp. 2400-2403.
4. **Ozin, G. A.** 2000, *Chem. Commun.*, pp. 419-432.
5. **Ungar, G., et al.** 2003, *Science*, pp. 299,1208-1211.
6. **Zuo, L., et al.** 2007, *Med. Clin. North Am.*, pp. 91, 845.
7. **Tseng, R. J., et al.** 2006, *Nature Nanotechnol.*, Vol. I, pp. 72-77.
8. **Royston, E., et al.** 24 (3), 2008, *Langmuir*, pp. 906-912.
9. **Tan, W.S., et al.** 24 (12), 2008, *Langmuir*, pp. 12483-12488.
10. **Rothmund, P.** 2006, *Nature*, Vol. 440, pp. 297-302.
11. **Knez, M., et al.** 3 No. 8, 2003, *Nanoletters*, pp. 1079-1082.
12. **Knez, M., et al.** 522, 2002, *Journal of Electroanalytical Chemistry* , pp. 70-74.
13. **Zaitlin, M.** 2000, *AAB Descriptions of Plant Viruses*, p. 370.
14. **Stubbs, G.** 1990, *Semin. Virol.*, Vol. I, pp. 405-412.
15. **Namba, K., Pattanayek, R. and Stubbs, G.** 208 (2), 1989, *J. Mol. Biol.*, pp. 307-325.
16. **Yi, H., Rubloff, G. and Culver, J.** 23 (5), 2007, *Langmuir*, pp. 2663-2667.
17. **Smolenska, L., et al.** 441, 1998, *FEBS Lett.*, p. 379.
18. **Schwyzer, R. and Kriwaczek, V. M.** 20, 1981, *Biopolymers*, pp. 2011-2020.
19. **Werner, S., et al.** 103, 2006, *Proc. Natl. Acad. Sci. U.S.A.*, pp. 17678-17683.